RADIATION DEPENDENCE OF DIVERTOR LEG LENGTH IN DETACHMENT ON DIII-D

[1]M.W. SHAFER, [2]A.G McLEAN, [3]A.W. LEONARD, [2]F. SCOTTI, [1]R.S. WILCOX

[1]Oak Ridge National Laboratory, Oak Ridge, TN, USA
[2]Lawrence Livermore National Laboratory, Livermore, CA, USA
[3]General Atomics, San Diego, CA, USA

Email: shafermw@ornl.gov

1. INTRODUCTION

Experiments performed on DIII-D demonstrate that extending the outer divertor leg allows for expanding the impurity radiation required for dissipation in detachment. This is roughly in line with convective transport estimates although deep detachment can lead toward radiation collapse to the X-point. Detachment is likely required for all future machines and understanding the interplay with confinement and detachment via radiation near the X-point is essential for projecting high confinement core edge integration that does not negatively impact pedestal stability and core performance.

Accommodating divertor radiation sufficient for detachment at the target surface requires understanding of each dissipation process taking place along a flux tube, each extending along a specific spatial extent through a range of T_e: impurity radiation from ~10-30 eV for carbon and nitrogen on machines like DIII-D, main ion ionization at ~5-10 eV, neutral interactions, charge exchange below ~5 eV, recombination below ~1 eV. For medium-Z radiators, impurity radiation is the highest-T_e dissipative process in detachment and the main driver to reduce T_e at the outer leg enabling the other dissipative processes. On DIII-D, whether it be intrinsically sputtered carbon or extrinsically puffed nitrogen, peak radiation density occurs at ~10 eV in the radiation loss parameter, $L_z = P_{rad}/n_e n_Z$. In detachment, parallel convection is found to dominate energy transport and define the spatial scale of impurity radiation where Mach 1 flow is inferred in the convective region [1]. Cross-field convective transport through drifts can still be a factor, but parallel convection dominates [2]. In this limit, the poloidal length needed to permit adequate impurity radiation can be estimated from the effective dissipation time, τ_{dis}, and sound speed, c_s. Here, $\tau_{dis} = E_{th}/P_{rad}$ where E_{th} is the thermal energy in the radiating volume. Using existing characterizations of the carbon concentration at detachment, the impurity radiation can be estimated leading to an effective length for impurity radiation to be defined as $L_{eff,\perp} = c_s \tau_{dis} \sin\theta$ where θ is the field line angle to the surface.

2. EXPERIMENTAL DATA

Experiments were performed on DIII-D employing small core volume plasmas in which the outer divertor leg length, L_{pol}, was extended up to 55 cm to test the estimates of the radiating volume in the convective limit. Injected power of up to 9 MW was applied in both the favorable and unfavorable drift directions in subsequent shots. Both main ion deuterium fueling and extrinsic nitrogen were used to access the detached state. Detachment was characterized by both a rollover in the ion saturation current at both targets plus measurements of the target $T_e < 2$ eV measured by divertor Thomson scattering at the outer target. Ultimately the outer leg length is found to play a minor role in detachment onset with L_{pol}=55 cm detaching at approximately 5% lower f_g than L_{pol}=35 cm with main ion gas puffing. The normalized confinement H_{98} drops from above 1 (peaking at 1.2) before detachment and drops below one, reducing as the divertor is driven deeper into detachment. The neutral compression (ratio of the neutral pressure at the midplane to the divertor in the private flux region) drops from ~5e4 to 1e4 when comparing L_{pol}=38 cm to L_{pol}=55 cm, although neutral compression is not lost in either case deep into detachment.

Radiated power is found to extend along the outer leg in detachment and can ultimately collapse to the X-point pushing into deep detachment. This can best be viewed examining the visible filtered CIII emission pattern via tangential imaging with high spatial resolution. While only a component of the overall radiated power, carbon radiation is the dominant radiator in the main ion fuelled detachment scans and remains significant even with nitrogen seeding. This is shown in Figure 2 for a main ion gas puffing scan. At the lowest density (left), the outer leg is attached, while the inner leg is detached. This state is typically found in most DIII-D discharges with B_T such that ion $B \times \nabla B$ drift is directed toward the divertor. With the inner leg detached, there is little change in confinement. Upon increasing density, the strong peak in CIII radiation at the target pulls away with some target radiation remaining due to ELMs. The radiation pattern is then found to extend along the outer leg with significant inner leg radiation near the X-point. Albeit lower intensity, this volume is still quite large. Pushing density higher shrinks that radiating region and eventually can push it into the confined region. The total radiated power (not shown) similarly extends along the outer leg but with lower spatial resolution and does not distinguish the inner/outer leg constituents well. Initial SOLPS-ITER simulations in Figure 1 show the total radiated power in similar conditions over a density scan. These simulations similarly show the extended radiation pattern along the outer leg at detachment onset and into the detached state, then being pushed deeper toward the X-point at higher density. These simulations will be used to further examine the influence of convection on the radiation pattern distribution when drifts are applied.

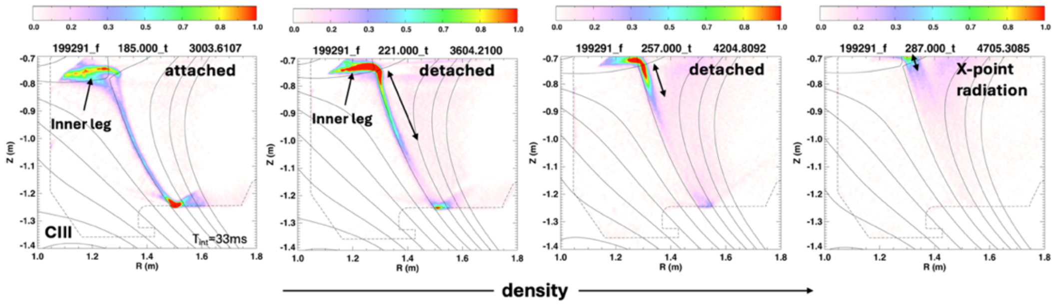

Figure 2 CIII emission showing outer leg radiation pattern in attached conditions and extending along the outer leg in detachment, ultimately shrinking toward the X-point in deeply driven detachment via main ion gas puffing.

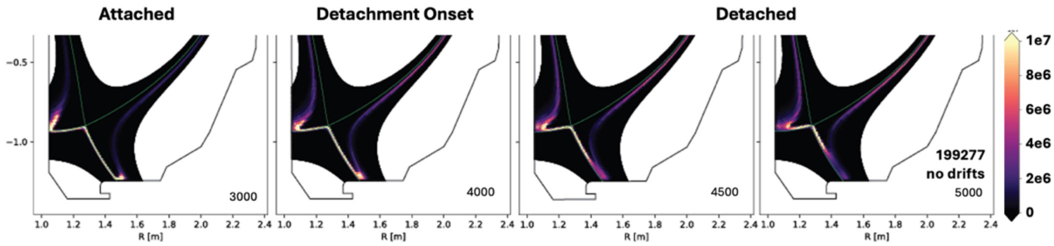

Figure 1 SOLPS-ITER simulations showing total radiated power extending along the outer leg in detachment.

3. CONCLUSION

Increasing the outer leg length alone helps to accommodate the dominant radiating impurities in detachment. The pattern extends along the outer leg. In the convective limit, this would be approximately 20 cm, which is on the scale of the results. Further simulations will better inform this picture and continued study on DIII-D will examine the role of baffling to impact impurity compression and flows. Determining the relative roles of dissipiation mechanisms is crucial, for future devices whose performance may depend on little to no core degradation in detachment.

ACKNOWLEDGEMENTS

This work was supported in part by the US Department of Energy under DE-AC05-00OR22725, DE-AC52-07NA27344, and DE-FC02-04ER54698.

REFERENCES

[1] A. W. Leonard, et. al, Phys. Rev. Lett. 78, 4769 (1997)

[2] A.E. Jaervinen, et. al, Contrib. Plasma Phys. 2020;60:e201900111